An accelerating precursor to predict "time-to-failure" in creep and volcanic eruptions

Shengwang Hao [a,b,*], Hang Yang [a], Derek Elsworth [c]

[a] *School of Civil Engineering and Mechanics, Yanshan University, Qinhuangdao, China*
[b] *The State Key Laboratory of Nonlinear Mechanics, Institute of Mechanics, Chinese Academy of Science, Beijing, China*
[c] *Energy and Mineral Engineering, Geosciences, G³ Center, EMS Energy Institute, Pennsylvania State University, University Park, PA, USA.*

A B S T R A C T

Real-time prediction by monitoring of the evolution of response variables is a central goal in predicting rock failure. A linear relation $\dot{\Omega}\,\ddot{\Omega}^{-1} = C\,(t_f - t)$ has been developed to describe the time to failure, where Ω represents a response quantity, C is a constant and t_f represents the failure time. Observations from laboratory creep failure experiments and precursors to volcanic eruptions are used to test the validity of the approach. Both cumulative and simple moving window techniques are developed to perform predictions and to illustrate the effects of data selection on the results. Laboratory creep failure experiments on granites show that the linear relation works well during the final approach to failure. For blind prediction, the simple moving window technique is preferred because it always uses the most recent data and excludes effects of early data deviating significantly from the predicted trend. When the predicted results show only small fluctuations, failure is imminent.

© 2017 Elsevier B.V. All rights reserved.

1. Introduction

Accelerating precursors exhibited by response quantities, such as strain, acoustic emission and seismic events, have been widely accepted as a significant way to predict the time-to-failure. Rates of ground deformation and of local fracturing of the crust or volcanic edifice (Voight, 1988; Cornelius and Voight, 1995; Kilburn and Voight, 1998; De la Cruz-Reyna and Reyes-Davila, 2001; Kilburn and Petley, 2003; Sparks, 2003; Smith et al., 2007; Lengliné et al., 2008; Bell and Kilburn, 2012; Kilburn, 2012; Boué et al., 2015; Salvage and Neuberg, 2016) commonly accelerate before volcanic eruptions. Accelerating creep deformation has also been suggested as a method to predict landslides (Saito, 1969; Kilburn and Petley, 2003; Petley et al., 2005). The "Voight" relation (Voight, 1988, 1989) describes the acceleration in terms of a self-accelerating process, given by:

$$\ddot{\Omega}\,\dot{\Omega}^{-\alpha} = A \qquad (1)$$

where Ω represents a response quantity and α and A are parameters. The overscripted dot and double-dot represent the rate and acceleration.

Such acceleration precursors have been confirmed in the laboratory (Cornelius and Scott, 1993; Lavallée et al., 2008; Heap et al., 2009; Smith et al., 2009; Kilburn, 2012; Hao et al., 2014; Bell et al., 2011a, 2011b; Vasseur et al., 2015). To provide insights into the accelerating behavior near the failure point, damage models have been developed to explain accelerating seismicity or deformation rates prior to rock failure (Main, 1999), volcanic eruptions (Kilburn and Petley, 2003), and landslides (Helmstetter et al., 2004). Together with time-dependent changes in applied stress and rock resistance, Kilburn (2012) proposed a model to extend analyses to deformation under increasing stress by accommodating changes with stress. He suggested an alternative expression to the Voight (1988, 1989) relation to describe how precursory time series can be determined from a relation between fracturing and stress.

A power law relation of the rates of response quantities with respect to the time-to-failure

$$\dot{\Omega} = k\,(t_f - t)^{-\beta} \qquad (2)$$

can be deduced from the Voight relation (1) (Voight, 1988, 1989; Main, 1999), where t_f is the failure time, $k = [A\,(\alpha - 1)]^{1/(1 - \alpha)}$ and $\beta = 1/(\alpha - 1)$ (Voight, 1989). This critical power law behavior has been demonstrated to be valid by observations for natural hazards such as landslides (Saito and Uezawa, 1961; Saito, 1969; Petley et al., 2002), volcanic (Voight, 1988), or cliff collapses (Amitrano et al., 2005), failure in laboratory creep (Nechad et al., 2005; Heap et al., 2009) and creep-relaxation experiments of rocks (Hao et al., 2014). Hao et al. (2013)

* Corresponding author at: School of Civil Engineering and Mechanics, Yanshan University, Qinhuangdao, China.
E-mail addresses: hsw@ysu.edu.cn (S. Hao), yh928@stumail.ysu.edu.cn (H. Yang), elsworth@psu.edu (D. Elsworth).

Table 1
Values of α measured in laboratory and field.

α	Loading conditions	References
1.66	Unknown	Voight, 1988
1.0		
1.97		
1.4		
~2.0		
~1.5		Cornelius and Voight, 1995
~2.0		Kilburn and Petley, 2003
1–3		Voight, 1989
~2.0		Kilburn and Petley, 2003
3.3		Smith & Kilburn (2010 Mount Pinatubo, 1991, 3 data points)
2.1		Smith & Kilburn (2010 Mount Pinatubo, 1991, 7 data points)
1.47–2.42	Constant load strain test	Cornelius and Scott, 1993
1.74–2.1	Constant stress	Voight, 1989
2.0		Heap et al., 2011
~2.96	Test by monotonically increasing the boundary displacement	Hao et al., 2013
~2.5	Creep-relaxation tests	Hao et al., 2014
3.0	Fiber bundle models loaded by increasing stress	Hao et al., 2016

introduced a response function as the change in the deformation of the sample with respect to the crosshead displacement of a testing machine, and found that the response function showed a critical power-law singularity at the failure point, where the crosshead displacement is a combination of the deformations of both the loading apparatus and the deformed sample, because they consist of a deforming system in series during the loading process.

Eqs. (1) and (2) have the interesting implication that, when $\beta = 1$ ($\alpha = 2$), the inverse rate decreases linearly with time:

$$\dot{\Omega}^{-1} = \frac{1}{k}\left(t_f - t\right) \tag{3}$$

Thus, by linearly extrapolating the curve of the inverse rate to zero, the failure time t_f can be determined as the intersection with the time axis (Voight, 1988, 1989; Kilburn and Voight, 1998; De la Cruz-Reyna and Reyes-Davila, 2001; Kilburn and Petley, 2003; Sparks, 2003; Smith et al., 2007; Lengliné et al., 2008; Lavallée et al., 2008; Bell and Kilburn, 2012; Kilburn, 2012), representing an infinite deformation rate. This method works well in retrospective prediction for such laboratory experiments, landslides, and volcanic eruptions (Voight, 1988; Cornelius and Voight, 1994, 1995; Kilburn and Voight, 1998; Murray and Ramirez Ruiz, 2002; Budi-Santoso et al., 2013).
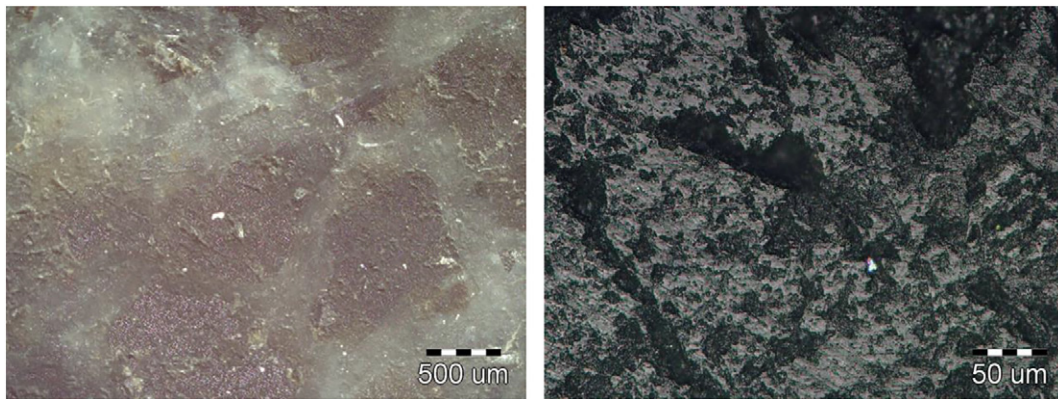
Fig. 1. Optical microscope images of a granite sample before loading.
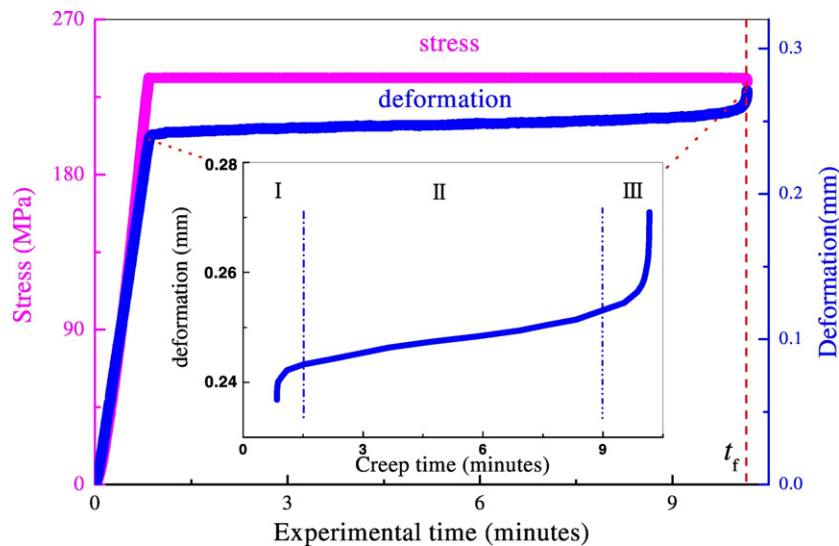
Fig. 2. Stress, strain versus time curves in a brittle creep experiment on the sample—granite-1. Stress: solid black line; Deformation: blue line. The loading process includes two phases: a phase of imposing an initial stress on the sample, and a constant stress (creep) phase. The inset shows a zoomed-in view to the creep phase.
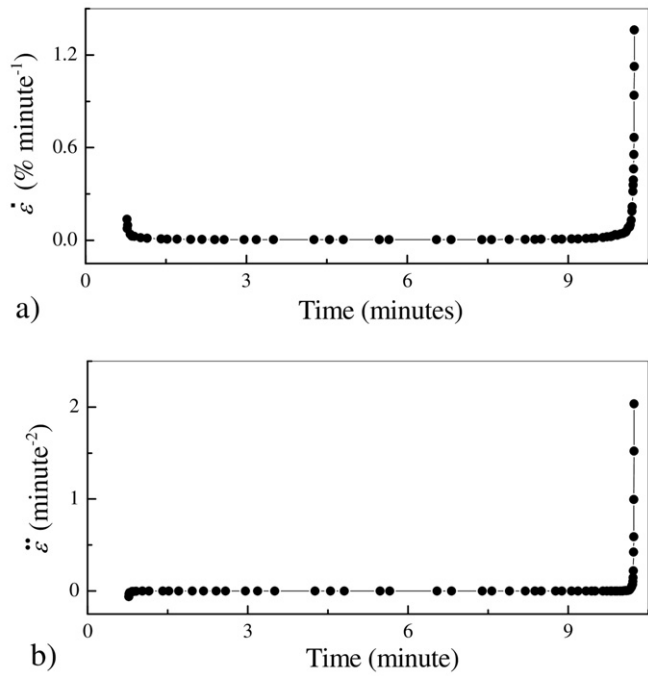
Fig. 3. Evolution of strain rate and acceleration for sample granite-1. a) Strain rate; b) Acceleration.

eruption (Philippines) and tend to 2.10 for 7 data points. Compressional deformation experiments on marble and granite (Hao et al., 2013) have shown that the average value of the power exponent β is 0.51 with a range from 0.37 to 0.72 ($\alpha = 2.96$ with a range from 2.39 to 3.70). For creep-relaxation experiments on rock, Hao et al. (2014) found that the exponent β is about 2/3 ($\alpha = 2.5$). Finally, in the analysis of viscoelastic fiber bundle models (Kun et al., 2003; Turcotte et al., 2003; Hao et al., 2012) $\beta = 0.5$ ($\alpha = 3$). It should also be noted that, whereas Voight (1988, 1989) originally proposed that precursory signals follow a single trend, an alternative view is that the trend evolves with time from conditions for $\alpha \approx 1$ to conditions for $\alpha \approx 2$ (Kilburn and Voight, 1998; Kilburn and Petley, 2003; Kilburn, 2012). Consequently, the uncertainty resulting from the scatter of exponents α (or β) is a key difficulty in using such methods for prediction of the failure time through the use of acceleration precursors.

An alternative relation (Hao et al., 2016)

$$\dot{\Omega}\,\ddot{\Omega}^{-1} = C\,(t_f - t) \tag{4}$$

was derived to describe the time to failure. $\dot{\Omega}\,\ddot{\Omega}^{-1}$ is the ratio of rate to acceleration of the response process, and $C = \alpha - 1$. The failure time can be determined by extrapolating the curve of $\dot{\Omega}\,\ddot{\Omega}^{-1}$ versus time to its intersection with the time axis. The advantage of this method is that the prediction can be performed without a need to know in advance the exponent α (or β).

In order to highlight the potential of predicting the failure time through monitoring the evolution of $\dot{\Omega}\,\ddot{\Omega}^{-1}$, this paper presents real-time prediction analyses using two data sets—(1) creep failure experiments on granites and (2) volcanic eruptions. In creep experiments, the complete evolution process of $\dot{\Omega}\,\ddot{\Omega}^{-1}$ is illustrated to show how it evolves to the critical linear relation. Two methods, here called the "cumulative" and "simple moving time window" techniques, are developed to predict the failure time t_f. For the method of the simple moving time window, only the recent data, up to the current time, are used to perform the prediction—the other previous data are ignored. The prediction is made step-by-step with time moving towards the failure time. Two volcanic data sets are then used to validate the application, before discussing the time scale that illustrates the failure precursors and the data selection for performing the prediction.

However, the exponent α is not always equal to 2 but exhibits variation. Table 1 lists some values of α measured in laboratory and field for a range of loading conditions. For example, slope failures analyzed by Voight (1989) encompassed the range $1 \leq \alpha < 3$. The eruptions yield $\alpha \approx 1.66$ (Voight, 1989) and 1.5 (Cornelius and Voight, 1995) for Bezymyanny, 1960 and Mount St. Helens, 1986, respectively. In constant load strain tests performed by Cornelius and Scott (1993), α ranged between 1.47 and 2.12. At Mount St. Helens volcano (Washington, USA) for deformations measured 1980 to 1986, α values were ~1.5 (Voight and Cornelius, 1991). Voight (1989) discovered that α is between 1.74 and 2.01 for failure experiments on alloys and metals, and ranges from 1.9 to 2.1 for soils. Smith and Kilburn (2010) found that α took values of up to 3.30 for 3 data points for the 1991 Mount Pinatubo

Fig. 4. Evolution curves of $\dot{\varepsilon}\,\ddot{\varepsilon}^{-1}$ versus time for three samples. a) Granite-1; b) Granite-2; c) Granite-3. The inset zooms-in on the linear relation nearby the failure time. Note that the early data deviate significantly from the critical linear relation. The vertical dashed line shows the failure time.
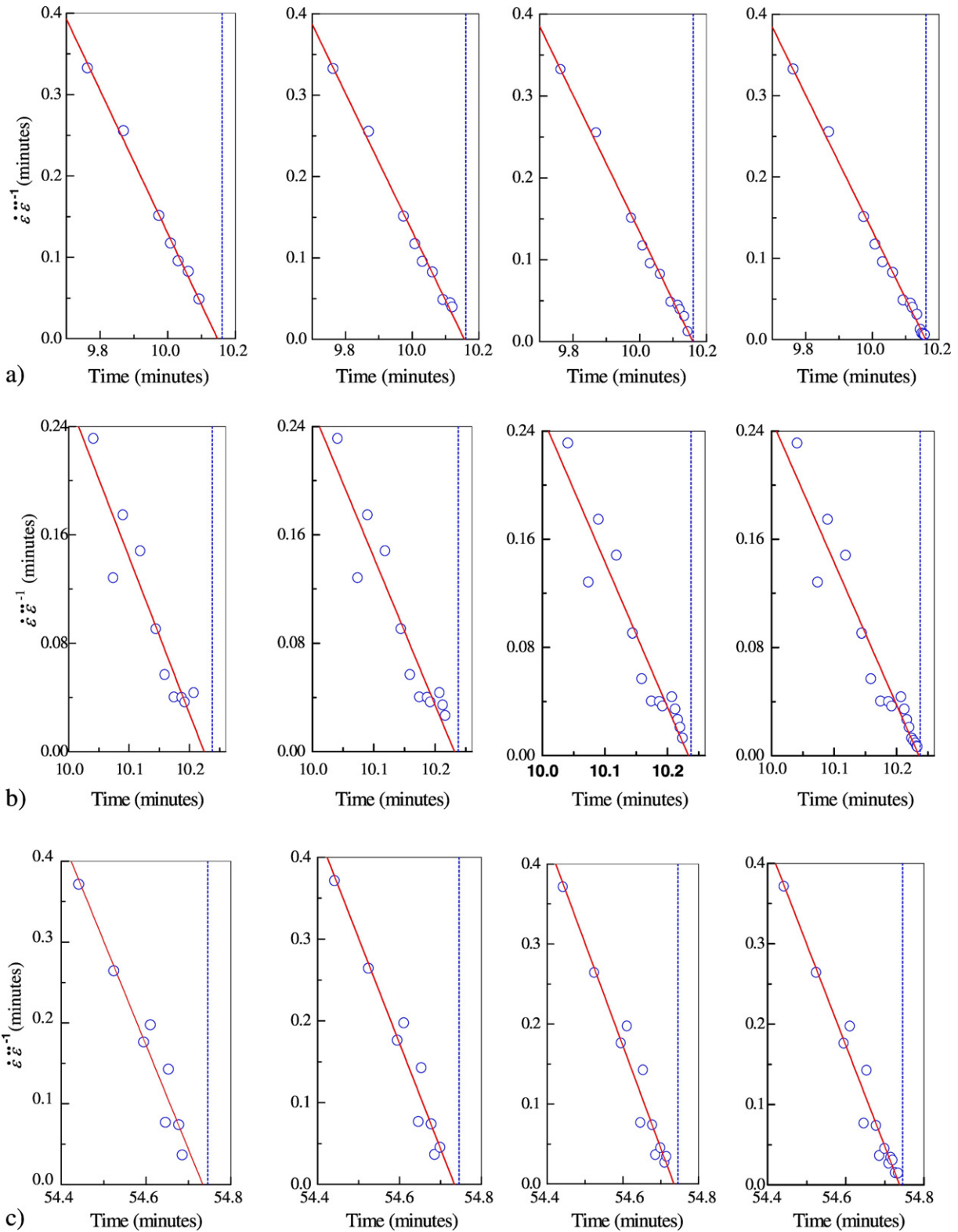
Fig. 5. Predicted results using the cumulative moving technique for three samples as examples. a) Granite-1; b) Granite-2; c) Granite-3. Every fitting starts from the same fixed point but ends at every individual time. Consequently, the number of data points used for fitting increase with time approaching the failure time. The solid lines are the fitted results and the intersection point with time axis is the predicted result. The vertical dashed line shows the real failure time.

2. Experimental methodology of creep failure experiments

Creep failure experiments were performed on prismatic granite blocks (Hao et al., 2014), where the rock specimen was first loaded to a prescribed initial stress and held at that constant stress to observe the evolution of deformation. The bulk density of the granite is 2.5 to 2.7 g/cm^3 and its water absorption is 0.16%, defined as mass of adsorbed water relative to unit mass of the dry rock. Fig. 1
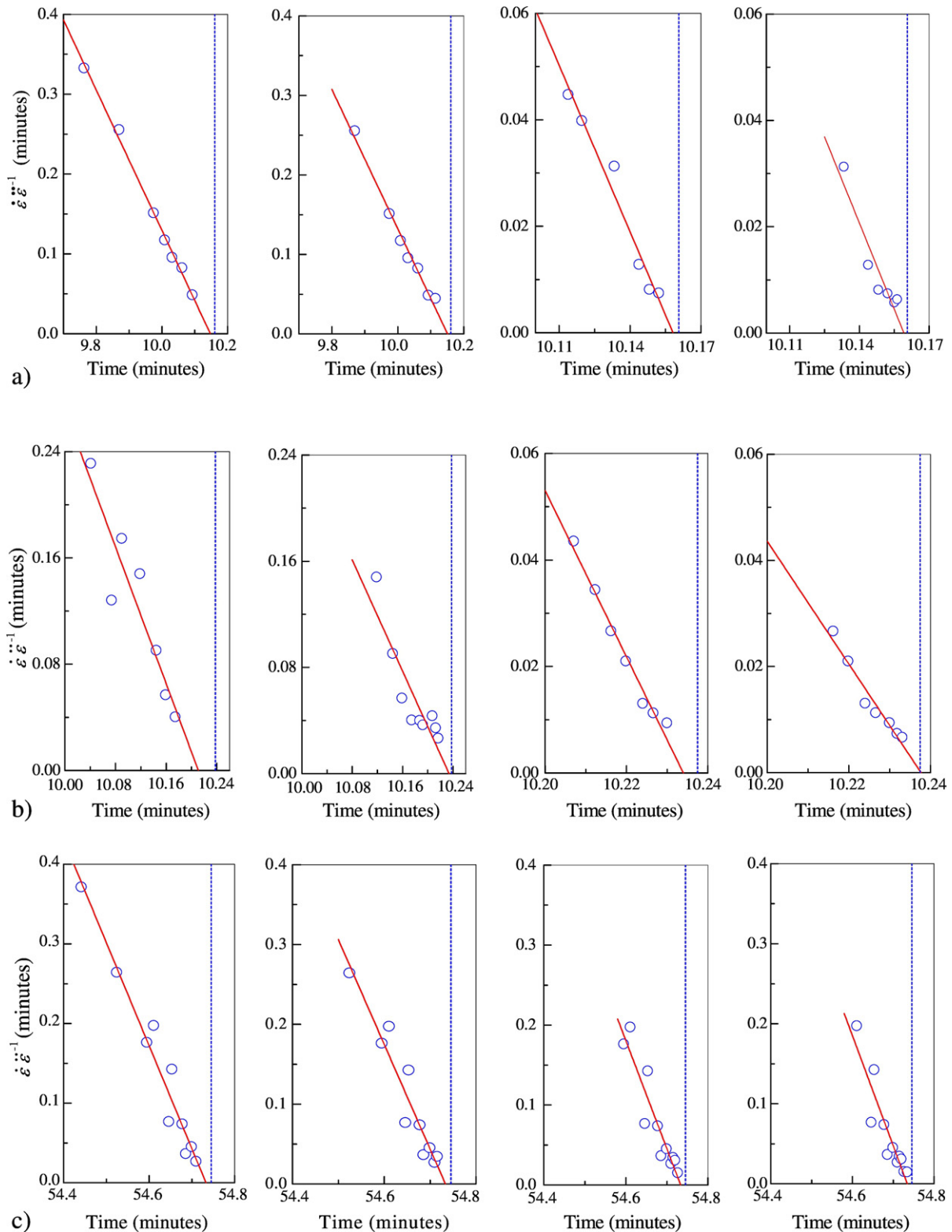
Fig. 6. Predicted results by using the simple moving window technique. a) Granite-1; b) Granite-2; c) Granite-3. During the process of fitting, only the most recent data (in a window) are used in the prediction, i.e. the starting and ending time of the data points used for the prediction are variable as a moving window. The solid lines are the fitted results and the intersection point with time axis is the predicted results. The vertical dashed line plots the real failure time.

presents two optical microscope images that show the internal structure and grain size and texture of the samples. The deformation, u, of the specimen was measured using 1 μm resolution extensometers (LVDT) located on the both sides of the specimen.

3. Evolution of strain, strain rate, acceleration and $\dot{\varepsilon}\,\ddot{\varepsilon}^{-1}$ in creep failure of granite

The experimental protocol is illustrated in Fig. 2 with the inset showing a plot of axial strain against time for the creep phase of the

Fig. 7. False-prediction produced by the cumulative moving technique for the sample—granite-3. The initial data, that do not show the critical linear response, will give a false-prediction earlier than the current time of the recent captured data, which clearly must deviate significantly from the real failure time. The vertical dashed line plots the real failure time.
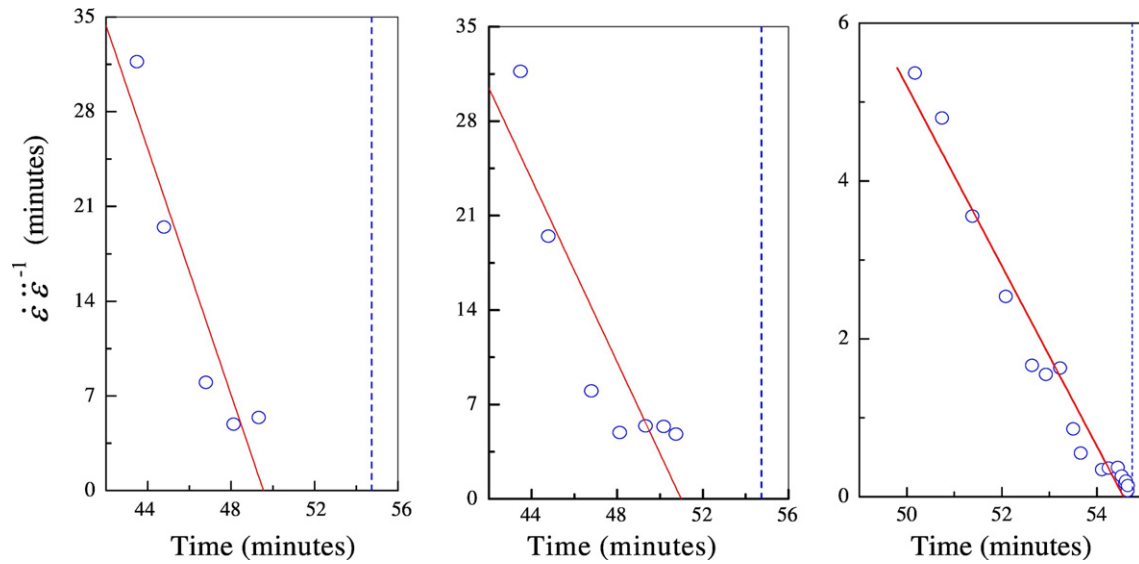
experiment. Fig. 3 shows the curves of strain, strain rate, and acceleration versus time for creep failure experiments for the sample shown in Fig. 2. Two typical processes are apparent: a strain deceleration following setting the load as constant and a final acceleration leading to failure. In both the decelerating and accelerating stages, the ratio $\dot{\varepsilon}\,\ddot{\varepsilon}^{-1}$ of strain rate to acceleration decreases with time (Fig. 4).

Whether a true steady state phase exists, with zero acceleration (constant rate), remains open to debate, and will be discussed in Section 6. In the present creep failure experiments, a phase is observed when the accelerations are very small. As a result, the scatter, caused by differentiating and inverting noisy data inevitably leads to large fluctuations of the values of $\dot{\varepsilon}\,\ddot{\varepsilon}^{-1}$. Thus, the values of $\dot{\varepsilon}\,\ddot{\varepsilon}^{-1}$ in this stage are not calculated. This paper focuses on the data relevant to strain increasing rapidly as the time of failure is approached.

During the tertiary stage before failure, both the strain rate and acceleration increase rapidly and $\dot{\varepsilon}\,\ddot{\varepsilon}^{-1}$ decreases monotonically from a high magnitude until failure. The final linear portion of $\dot{\varepsilon}\,\ddot{\varepsilon}^{-1}$ near failure time (Fig. 4) demonstrates that Eq. (4) is appropriate for these experiments. The deviation of previous data from the final linear trend (Fig. 4) indicates that the acceleration process should be sub-divided into two parts with only the final culminating part described by Eq. (4) and acting as a failure precursor.

4. Predicting creep failure time in laboratory experiments on granite

Because Eq. (4) describes the trend close to failure time, only data near this time are used for the predictions. The failure time is assumed to be unknown and only the data preceding an individual time t^* are used in the projection—all "future" data are ignored—allowing a true prediction to be made. A linear least-squares method is used to obtain the best fit linear trend until t^*. The trend is then extrapolated to determine the predicted failure time.

To examine the effects of data point selection on the predicted results, two methods are used: one using all data points, and beginning from some fixed point; and the other using only the most recent data points. In the first method, designated as the "*cumulative time technique*", every fitting starts from the same fixed point but ends at every individual time t^*. Consequently, the number of data points used for fitting increases with t^* as it approaches the failure time. In the second method, referred to as the "*simple moving time window technique*", only the most recent data (in a window) are used, so that the difference between the start and

end time varies as the window moves. In both methods, the linear fitting is made stepwise with t^* moving to the failure time.

The two methods are illustrated for three experiments in Figs. 5 and 6. Both methods result in similar estimates that are very close to the real failure time. For the cumulative moving technique, including the most recent data slightly improves the agreement between the estimated and actual failure times (see Fig. 5a, b, c). The simple moving time window technique (Fig. 6a, b, c) also shows only small fluctuations in the estimated failure time. Both methods thus provide stable predictions of the failure time. Data should therefore be obtained as early as possible in order to improve the reliability of the prediction, and allow an earlier warning to be released. The stability of the results further demonstrates that the linear relation of Eq. (4) performs well as a "failure precursor".

The predictions are performed in hindsight because the data used for prediction are recognized as a failure precursor that can be described by Eq. (4). In practical applications, it is difficult to determine in advance whether the data are close to the failure time. Thus, we perform a prediction as soon as $\dot{\varepsilon}\,\ddot{\varepsilon}^{-1}$ begins to decrease. From Fig. 4, it is apparent that the initial data that do not show the critical linear response will give an estimation that deviates significantly from the real failure time—although they would have predicted a time still in the future. Importantly, the cumulative technique, including the initial data, sometimes produces an obvious mis-prediction that the predicted failure time is even earlier than the current time t^* (Fig. 7). The initial data that do not show the critical linear response are included in the prediction in Fig. 7—thus the ranges of values on the y-axis (strain velocity/acceleration) is about 32 min—that is about 100 times of that (<0.4 min) in Fig. 6c. In contrast, the simple moving technique returns an improved warning, because it always uses the most recent data. When the predicted results change little with time, failure is close and will occur close to the predicted time.

5. Prediction applied to volcanic eruption

Two data sets are used to demonstrate the application to both methods to volcanic eruptions. Data are used from (i) tiltmeter FAMOUS during the growth of a lava dome at Mount St. Helens in October 1986 (Cornelius and Voight, 1995), and (ii) seismic energy release before the eruption (t_e) of Bezymyanny Volcano from 1960 (Voight, 1988). Data used for predictions range from about a month before eruption for Mount St. Helens to about eight days prior for Bezymyanny.

Figs. 8 and 9 show the results for both events. Both the cumulative and simple moving techniques give similar results that are earlier by <2 days than the actual eruption time. These predicted results are as good and stable as the classical FFM (Voight, 1988; Cornelius and Voight, 1995). The data series in Figs. 8 and 9 present an almost identical prediction of failure time. Both techniques indicate that the data approaching failure change little with the approach to failure, allowing prediction via the linear relation fitted through the previous data. Thus, the linear relation of Eq. (4) works well for both data sets of volcanic eruptions and gives a robust warning.

6. Discussion

6.1. Onset of acceleration and warning precursors

It is not straightforward to determine the actual time when strain acceleration begins. Kranz and Scholz (1977) and Baud and Meredith (1997) reported that a critical level of volumetric strain is required to induce tertiary creep, whereas Heap et al. (2009) argue a critical amount of damage must be exceeded. However, it remains controversial as to whether there is a steady state stage between the accelerating and decelerating phases. Ngwenya et al. (2001) and Yang and Jiang (2010) argue that the secondary stage is not strictly a 'steady-state' process. Changes in porosity and acoustic emission in brittle creep experiments on basalt (Heap et al., 2011) show that damage increases throughout the secondary creep phase. We suggest that damage during the secondary stage is randomly distributed micro-damage, which has a minimal effect on the broad trend of macroscopic averaged response variables, such as the global average strain.

An almost linear secondary creep stage (or stable stage) is usually observed in rock creep experiments. In the present experiments, this is confirmed by a horizontal portion on the strain rate versus time curve (Fig. 3). During this stage, the acceleration in strain remains small but finite. It should be noted that it is almost impossible to obtain zero acceleration because of the errors resulting from the differentiation of noisy data, and so it is difficult to definitively determine whether the strain changes directly from deceleration to acceleration without passing through a steady stage.
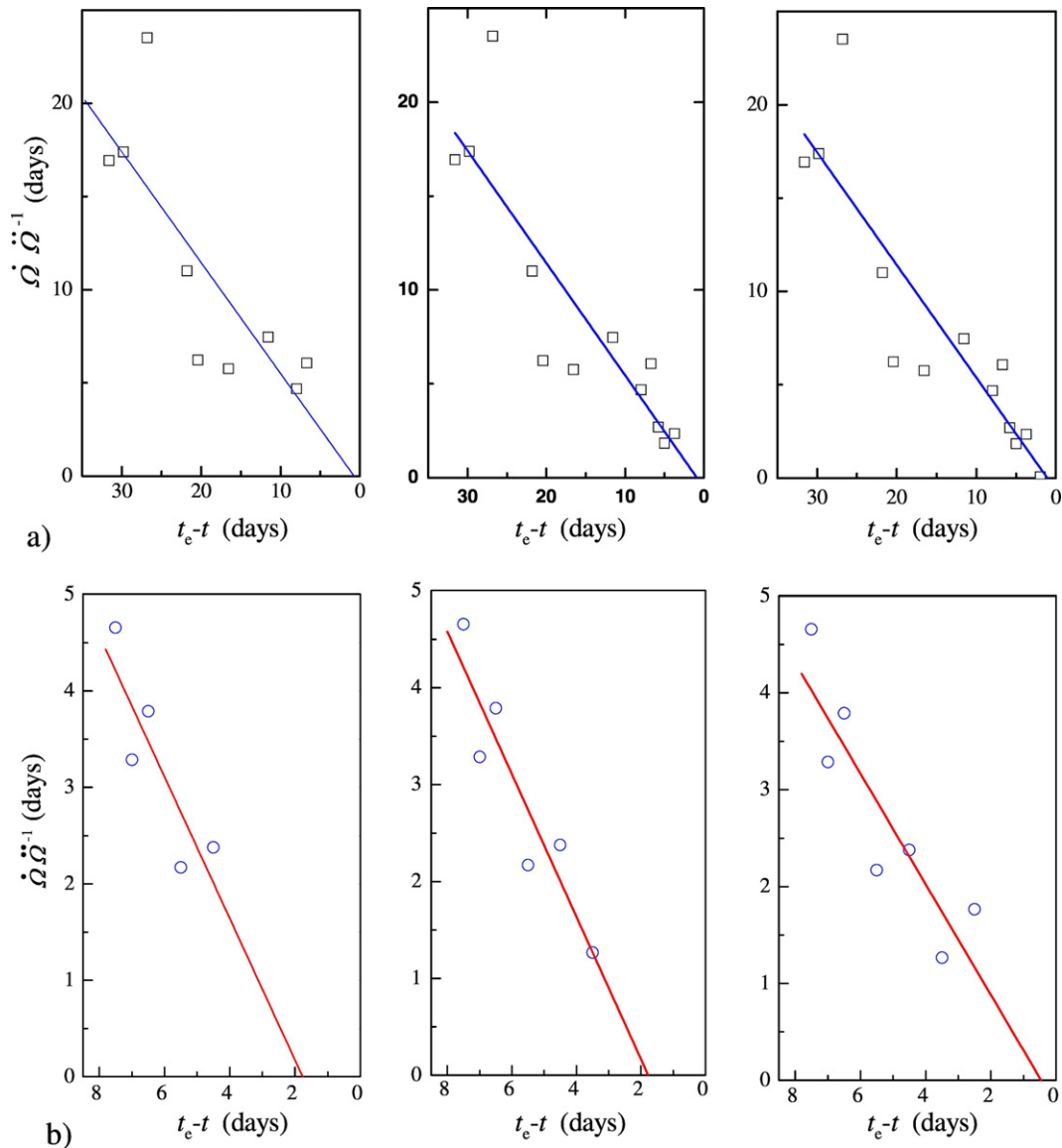
Fig. 8. Predicted process and results of volcanic eruptions using the cumulative moving technique. a) Seismic energy release before eruption time (t_e) (Voight, 1988), Bezymyanny Volcano, 1960. Ω = cumulative seismic strain release (10^3 J$^{1/2}$). b) Data from tiltmeter FAMOUS at Mount St. Helens (Cornelius and Voight, 1995), October 1986. Ω = tilt (μrad). The extrapolation of fitting lines gives a failure prediction <2 days earlier than the actual eruption time. When the data points increase to closer to the failure time, there is little change on the failure prediction. Thus, it presents a robust warning of the failure time.
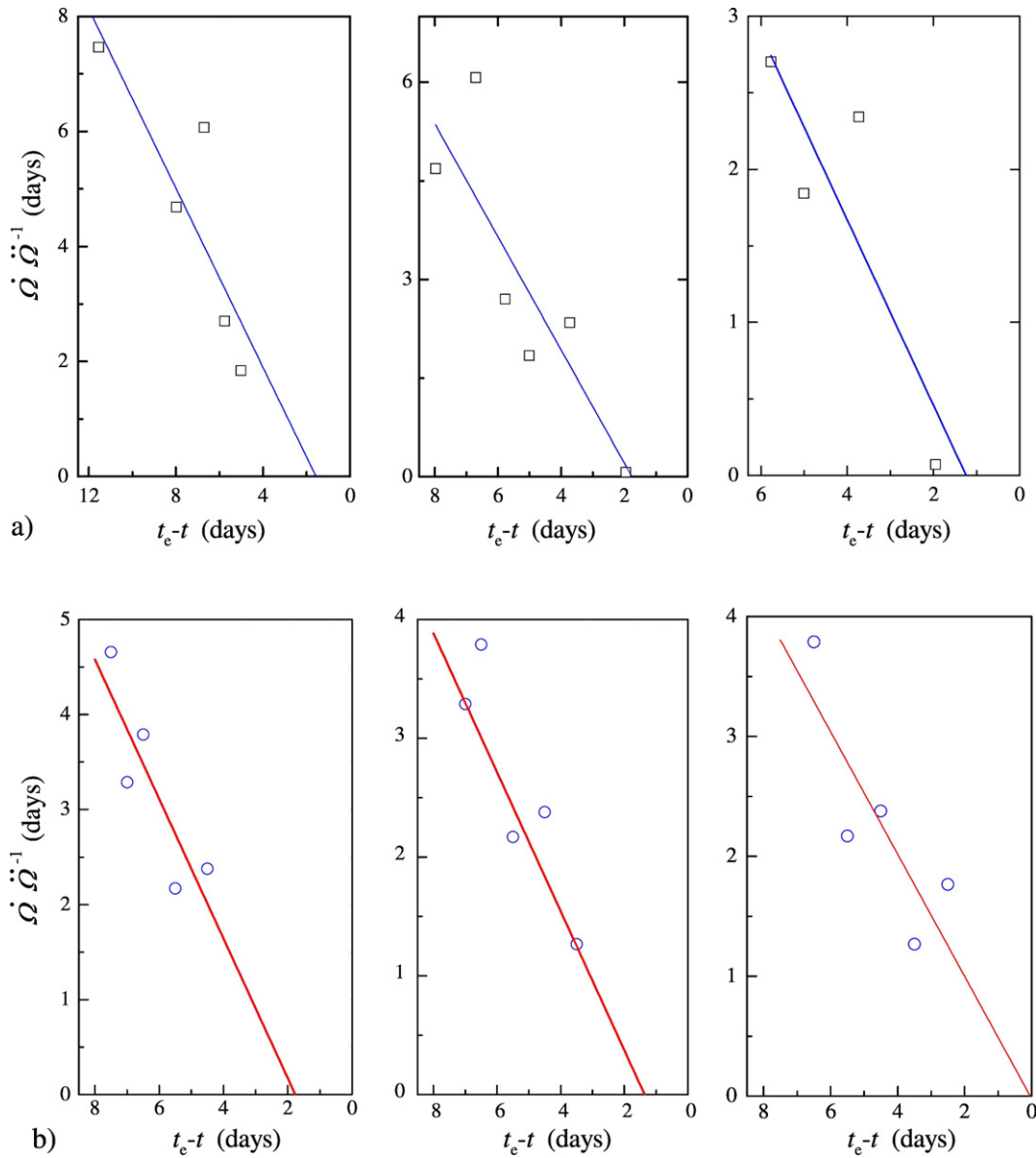
Fig. 9. Predicted process and results of volcanic eruptions using the simple moving technique. a) Seismic energy release before eruption time (t_e) (Voight, 1988), Bezymyanny Volcano, 1960. Ω = cumulative seismic strain release (10^3 J$^{1/2}$). b) Data from tiltmeter FAMOUS at Mount St. Helens (Cornelius and Voight, 1995), October 1986. Ω = tilt (μrad). The extrapolation of fitting lines gives a failure prediction that is earlier <2 days than the actual eruption. With the fitting window moving to the failure time, predictions create a robust warning of failure time.

The inevitable fluctuation in the rate and acceleration data, resulting from the differentiation of the original noisy data is the main cause of scatter in $\dot{\varepsilon}\,\ddot{\varepsilon}^{-1}$. In particular, $\dot{\varepsilon}\,\ddot{\varepsilon}^{-1}$ shows a larger scatter during the secondary stage and the early phase of the tertiary stage due to the low magnitude of the accelerations. Only data close to the time of failure form a linear trend on the curve of $\dot{\varepsilon}\,\ddot{\varepsilon}^{-1}$. The decreasing trend of the earlier data clearly deviates from this linear trend. Thus, the tertiary stage may be divided into two parts, with only the final part described by a linear trend and capable of extrapolation as a precursory warning. For data from tiltmeter FAMOUS at Mount St. Helens (Cornelius and Voight, 1995), October 1986, only data later than 8 days conform to the critical linear relation (Fig. 10).

6.2. Datum point selection for prediction

Some data on the curve of $\dot{\Omega}\,\ddot{\Omega}^{-1}$ may significantly bias the prediction from the global trend. For example, two data points 20 to 15 days before the 1960 eruption of Bezymyanny Volcano (Voight, 1988), deviate significantly from the global trend. The time prediction from data ending at these two data points is significantly earlier than the actual eruption (Fig. 11a). The results predicted from data starting at these two locations in the time series are dangerous/non-conservative as the prediction time is much later than the actual time of eruption (Fig. 11b). So in its application, the data should be assigned to exclude these data as non-representative. But the remaining data, immediately before failure present a consistency of the linear trend with small deviation, and thus provide a good warning.

Only data close to failure time can be described by Eq. (4). For the cumulative fitting method, the starting point of the data has a significant influence on the predicted results. It is difficult to blindly determine data close to the failure time. However, these data have little influence on the simple moving window fitting method because it always uses only the most recent data. The number of data points used in the calculation becomes a key influence on the precision of the prediction. Consequently, it is better to change the number of data points, i.e.
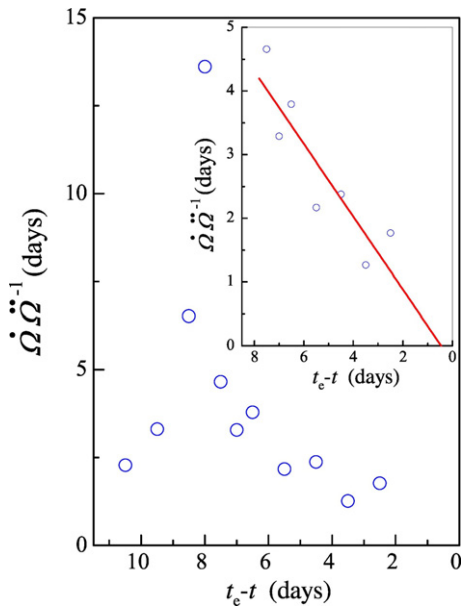
Fig. 10. Evolution curves of $\dot{\Omega}\,\ddot{\Omega}^{-1}$ versus time for data from tiltmeter FAMOUS at Mount St. Helens (Cornelius and Voight, 1995), October 1986. Ω = tilt (μrad). The inset zooms-in on the linear relation nearby the time of eruption. The early data before 8 days deviate significantly from the critical linear relation.

changing the start and end time for every fitting, in real-time, according to the trend exhibited by the acquired data.

6.3. Limits and methods of performing prediction from accelerating rates

For both the classical FFM (Voight, 1988, 1989; Kilburn and Voight, 1998; De la Cruz-Reyna and Reyes-Davila, 2001; Kilburn and Petley, 2003; Sparks, 2003; Smith et al., 2007; Lengliné et al., 2008; Lavallée et al., 2008; Bell et al., 2011a, 2011b, 2013; Bell and Kilburn, 2012;

Kilburn, 2012; Boué et al., 2015; Salvage and Neuberg, 2016) and the present method, the signal has to be differentiated with respect to time and inverted, hence large fluctuations introduced by these operations pose an important limitation in terms of real-time operational usage. In the relation of Eq. (4), the parameter $C = \alpha - 1$ is the slope of the fitted line. In order to compare this with the classic FFM and to confirm the observed trends, the curves of acceleration versus rate for three samples and the values of α are illustrated in Fig. 12. It can be seen that the values of C in the present method agree well with the values of α in the classic FFM.

For point data, such as seismic events, a method developed in Bell et al. (2013) alleviates such a limitation by relying on the most raw data possible (i.e. the individual timings of the events) through the use of a likelihood function. However, it is not possible to use this method for continuous deformation data, and one would instead rely on the method developed in Bell et al. (2011a, 2011b) in which a GLM (Global Linearized Model) is applied to the unprocessed signal rate.

Our new method provides a mechanism to perform the prediction without the premise of knowing the exponent beforehand. The failure time can be estimated directly through monitoring the evolution of the response quantity, i.e. $\dot{\Omega}\,\ddot{\Omega}^{-1}$. However, the acceleration of the precursory signal (with time) must be calculated, and is thus expected to be associated with larger combined errors that may induce larger fluctuations. Further work, for example through synthetic tests and statistical analyses (cf. Bell et al., 2011a, 2011b), are needed to compare the efficacy between the present method and the classical FFM.

It should be mentioned that the proposed model identifies conditions for bulk failure, and not for an eruption. Once bulk failure occurs, magma will need time to ascend to the surface. Model failure times are thus expected to occur before observed eruption times. In the present paper, field data for two eruptions have been compared with the results from creep tests in the laboratory. However, additional loading conditions may also occur before eruption (Kilburn, 2012). Further investigation is required to reveal whether the observed trends or the values of the exponent α depend on loading condition.
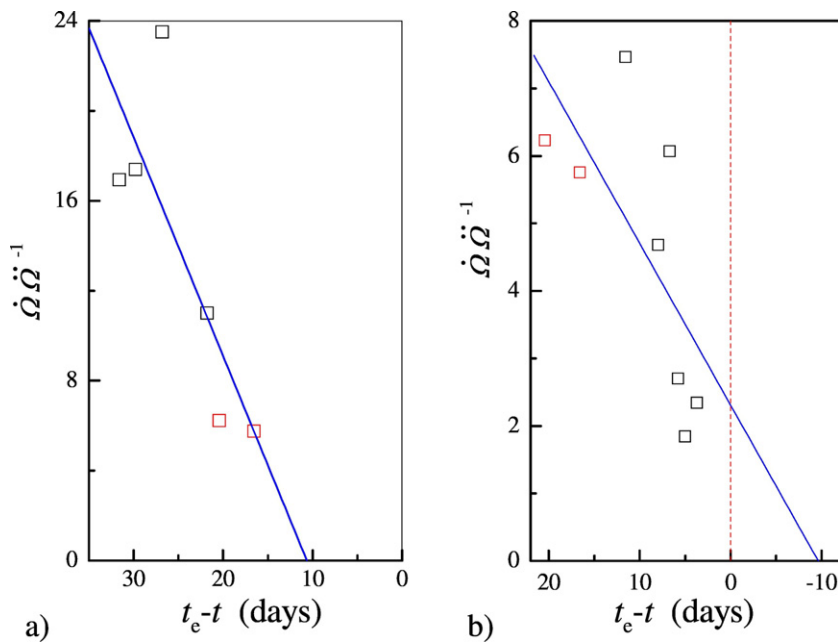
Fig. 11. Time to failure results predicted from the data either starting or ending at the two data points (illustrated by the red color) that deviate significantly from the main trend. Data are for seismic energy release before eruption time (t_e) (Voight, 1988), Bezymyanny Volcano, 1960. Ω = cumulative seismic strain release (10^3 J$^{1/2}$). a) The time prediction by data ending at these two data points with large deviations from the trend predict a very premature eruption. b) The eruption time prediction from data starting at these two data points is much later than the actual eruption time—an unconservative and dangerous prediction.

Fig. 12. Evolution curves of acceleration versus rate and the values of α for three samples. a) Granite-1; b) Granite-2; c) Granite-3.

7. Conclusions

A critical linearized relation Eq. (4) is shown to work well for measured creep failure and volcanic eruption data. The tertiary stage of deformation can be divided into two different phases. Not all of the data in the acceleration stage are useful for predicting failure time; only late-time data are useful.

The method gives a good prediction for the time to creep failure and for some volcanic eruptions. The predicted results are generally slightly earlier than the real time-to-failure, and thus can warn of the impending failure. During the final phase of the accelerating stage, the data in the time sequences give almost the same prediction by each of the methods proposed. Thus, it is better to capture the data as early as possible to provide the earliest possible warning of the failure time.

For blind predictions, the simple moving technique is more suitable for practical applications. This process uses only the most recent data, and excludes the influence of data that deviate significantly from the critical linear trend Eq. (4). When the predicted results change little with time, failure is imminent and will occur almost at the predicted time. However, calculations using differentiation of noisy data and inversion sometimes result in a large scatter in some data and it is important to not use these data as starting or ending data for performing the prediction.

References

Amitrano, D., Grasso, J.R., Senfaute, G., 2005. Seismic precursory patterns before a cliff collapse and critical point phenomena. Geophys. Res. Lett. 32 (5):L08314. http://dx.doi.org/10.1029/2004GL022270.

Baud, P., Meredith, P., 1997. Damage accumulation during triaxial creep of darley dale sandstone from pore volumetry and acoustic emission. Int. J. Rock Mech. Min. Sci. Geomech. Abstr. 34 (3–4), 1–8.

Bell, A.F., Kilburn, C.R.J., 2012. Precursors to dyke-fed eruptions at basaltic volcanoes: insights from patterns of volcano-tectonic seismicity at Kilauea volcano, Hawaii. Bull. Volcanol. 74, 325–339.

Bell, A.F., Greenhough, J., Heap, M.J., Main, I.G., 2011a. Challenges for forecasting based on accelerating rates of earthquakes at volcanoes and laboratory analogues. Geophys. J. Int. 185, 718–723.

Bell, A.F., Naylor, M., Heap, M.J., Main, I.G., 2011b. Forecasting volcanic eruptions and other material failure phenomena: an evaluation of the failure forecast method. Geophys. Res. Lett. 38 (15), L15304.

Bell, A.F., Naylor, M., Main, I.G., 2013. The limits of predictability of volcanic eruptions from accelerating rates of earthquakes. Geophys. J. Int. 194 (3), 1541–1553.

Boué, A., Lesage, P., Cortés, G., Valette, B., Reyes-Dávila, G., 2015. Real-time eruption forecasting using the material Failure Forecast Method with a Bayesian approach. J. Geophys. Res. 120 (4), 2143–2161.

Budi-Santoso, A., Lesage, P., Dwiyono, S., Jousset, P., Métaxian, J.P., 2013. Analysis of the seismic activity associated with the 2010 eruption of Merapi Volcano, Java. J. Volcanol. Geotherm. Res. 261, 153–170.

Cornelius, R.R., Scott, P.A., 1993. A materials failure relation of accelerating creep as empirical description of damage accumulation. Rock Mech. Rock. Eng. 26, 233–252.

Cornelius, R., Voight, B., 1994. Seismological aspects of the 1989–1990 eruption at Redoubt Volcano, Alaska: the materials Failure Forecast Method (FFM) with RSAM and SSAM seismic data. J. Volcanol. Geotherm. Res. 62, 469–498.

Cornelius, R., Voight, B., 1995. Graphical and PC-software analysis of volcano eruption precursors according to the materials Failure Forecast Method (FFM). J. Volcanol. Geotherm. Res. 64, 295–320.

De la Cruz-Reyna, S., Reyes-Davila, G.A., 2001. A model to describe precursory material-failure phenomena: applications to short-term forecasting at Colima volcano. Mex. Bull. Volcanol. 63 (5), 297–308.

Hao, S.W., Zhang, B.J., Tian, J.F., 2012. Relaxation creep rupture of heterogeneous material under constant strain. Phys. Rev. E 85 (1), 012501.

Hao, S.W., et al., 2013. Power-law singularity as a possible catastrophe warning observed in rock experiments. Int. J. Rock Mech. Min. Sci. 60, 253–262.

Hao, S.W., Zhang, B.J., Tian, J.F., Elsworth, D., 2014. Predicting time-to-failure in rock extrapolated from secondary creep. J. Geophys. Res. Solid Earth 119:1942–1953. http://dx.doi.org/10.1002/2013JB010778.

Hao, S.W., Liu, C., Lu, C.S., Elsworth, D., 2016. A relation to predict the failure of materials and potential application to volcanic eruptions and landslides. Sci. Rep. 6, 27877. http://dx.doi.org/10.1038/srep27877.

Heap, M.J., Baud, P., Meredith, P.G., Bell, A.F., Main, I.G., 2009. Time-dependent brittle creep in Darley Dale sandstone. J. Geophys. Res. 114, B07203. http://dx.doi.org/10.1029/2008JB006212.

Heap, M.J., et al., 2011. Brittle creep in basalt and its application to time-dependent volcano deformation. Earth Planet. Sci. Lett. 307 (1–2), 71–82.

Helmstetter, A., et al., 2004. Slider block friction model for landslides: application to Vaiont and la Clapière landslides. J. Geophys. Res. 109, B02409. http://dx.doi.org/10.1029/2002JB002160.

Kilburn, C.R.J., 2012. Precursory deformation and fracture before brittle rock failure and potential application to volcanic unrest. J. Geophys. Res. 117, B02211. http://dx.doi.org/10.1029/2011JB008703.

Kilburn, C.R.J., Petley, D.N., 2003. Forecasting giant, catastrophic slope collapse: lessons from Vajont, northern Italy. Geomorphology 54 (1–2):21–32. http://dx.doi.org/10.1016/S0169-555X(03)00052-7.

Kilburn, C.R.J., Voight, B., 1998. Slow rock fracture as eruption precursor at Soufriere Hills volcano, Montserrat. Geophys. Res. Lett. 25 (19), 3665–3668.

Kranz, R.L., Scholz, C.H., 1977. Critical dilatant volume of rocks at the onset of tertiary creep. J. Geophys. Res. 82 (30), 4893–4898.

Kun, F., Hidalgo, R.C., Herrmann, H.J., Pal, K.F., 2003. Scaling laws of creep rupture of fiber bundles. Phys. Rev. E 67, 061802.

Lavallée, Y., et al., 2008. Seismogenic lavas and explosive eruption forecasting. Nature 453 (7194):507–510. http://dx.doi.org/10.1038/nature06980.

Lengliné, O., et al., 2008. Seismicity and deformation induced by magma accumulation at three basaltic volcanoes. J. Geophys. Res. 113, B12305. http://dx.doi.org/10.1029/2008JB005937.

Main, I.G., 1999. Applicability of time-to-failure analysis to accelerated strain before earthquakes and volcanic eruptions. Geophys. J. Int. 139, F1–F6.

Murray, J., Ramirez Ruiz, J., 2002. Long-term predictions of the time of eruptions using remote distance measurement at Volcán de Colima, Mexico. J. Volcanol. Geotherm. Res. 117, 79–89.

Nechad, H., Helmstetter, A., El Guerjouma, R., Sornette, D., 2005. Creep ruptures in heterogeneous materials. Phys. Rev. Lett. 94, 045501.

Ngwenya, B.T., Main, I.G., Elphick, S.C., Crawford, B.R., Smart, B.G.D., 2001. A constitutive law for low-temperature creep of water-saturated sandstones. J. Geophys. Res. 106, 21811–21826.

Petley, D., Bulmer, M., Murphy, W., 2002. Patterns of movement in rotational and translational landslides. Geology 30 (8), 719–722.

Petley, D.N., Higuchi, T., Petley, D.J., Bulmer, M.H., Carey, J., 2005. Development of progressive landslide failure in cohesive materials. Geology 33 (3):201–204. http://dx.doi.org/10.1130/G21147.1.

Saito, M., 1969. Forecasting time of slope failure by tertiary creep. Proceedings of 7th International Conference on Soil Mechanics and Foundation Engineering, Mexico, pp. 677–683.

Saito, M., Uezawa, H., 1961. Failure of soil due to creep. Proc. 5th Int. Conf. Soil Mech. and Found. Eng., Montreal 1, pp. 315–318.

Salvage, R., Neuberg, J.W., 2016. Using a cross correlation technique to refine the accuracy of the Failure Forecast Method: application to Soufrière Hills volcano, Montserrat. J. Volcanol. Geotherm. Res. 324, 118–133.

Smith, R., Kilburn, C.R.J., 2010. Forecasting eruptions after long repose intervals from accelerating rates of rock fracture: the June 1991 eruption of Mount Pinatubo, Philippines. J. Volcanol. Geotherm. Res. 191:129–136. http://dx.doi.org/10.1016/j.jvolgeores.2010.01.006.

Smith, R., Kilburn, C.R.J., Sammonds, P.R., 2007. Rock fracture as a precursor to lava dome eruptions at Mount St. Helens from June 1980 to October 1986. Bull. Volcanol. 69 (6): 681–693. http://dx.doi.org/10.1007/s00445-006-0102-5.

Smith, R., Sammonds, P.R., Kilburn, C.R.J., 2009. Fracturing of volcanic systems: experimental insights into pre-eruptive conditions. Earth Planet. Sci. Lett. 280 (1–4): 211–219. http://dx.doi.org/10.1016/j.epsl.2009.01.032.

Sparks, R.S.J., 2003. Forecasting volcanic eruptions. Earth Planet Sci. Lett. 210 (1–2):1–15. http://dx.doi.org/10.1016/S0012-812X(03)00124-9.

Turcotte, D.L., Newman, W.I., Shcherbakov, R., 2003. Micro and macroscopic models of rock fracture. Geophys. J. Int. 152, 718–728.

Vasseur, J., et al., 2015. Heterogeneity: the key to failure forecasting. Sci Rep 5, 13259.

Voight, B., 1988. A method for prediction of volcanic eruptions. Nature 332:125–130. http://dx.doi.org/10.1038/332125a0.

Voight, B., 1989. A relation to describe rate-dependent material failure. Science 243, 200–203.

Voight, B., Cornelius, R.R., 1991. Prospects for eruption prediction in near real-time. Nature 350, 695–698.

Yang, S., Jiang, Y., 2010. Triaxial mechanical creep behaviour of sandstone. Min. Sci. Technol. 20, 339–349.